

## Cyanobacteria cause black staining of the National Museum of the American Indian Building, Washington, DC, USA

Francesca Cappitelli<sup>a\*</sup>, Ornella Salvadori<sup>b</sup>, Domenico Albanese<sup>c</sup>, Federica Villa<sup>a</sup> and Claudia Sorlini<sup>a</sup>

<sup>a</sup>Dipartimento di Scienze e Tecnologie Alimentari e Microbiologiche, Università degli Studi di Milano, Via Celoria 2, 20133 Milan, Italy; <sup>b</sup>Soprintendenza speciale per il patrimonio storico, artistico ed etnoantropologico e per il polo museale della città di Venezia e dei comuni della Gronda lagunare, Laboratorio Scientifico, Cannaregio 3553, 30131 Venezia, Italy; <sup>c</sup>Dipartimento di Chimica Organica e Industriale, Università degli Studi di Milano, via Venezian 21, 20133 Milan, Italy

(Received 10 December 2011; final version received 22 February 2012)

Microbial deterioration of stone is a widely recognised problem affecting monuments and buildings all over the world. In this paper, dark-coloured staining, putatively attributed to microorganisms, on areas of the National Museum of the American Indian Building, Washington, DC, USA, were studied. Observations by optical and electron microscopy of surfaces and cross sections of limestone indicated that biofilms, which penetrated up to a maximum depth of about 1 mm, were mainly composed of cyanobacteria, with the predominance of *Gloeocapsa* and *Lyngbya*. Denaturing gradient gel electrophoresis analysis revealed that the microbial community also included eukaryotic algae (Trebouxiophyceae) and fungi (Ascomycota), along with a consortium of bacteria. Energy-dispersive X-ray spectroscopy analysis showed the same elemental composition in stained and unstained areas of the samples, indicating that the discolouration was not due to abiotic chemical changes within the stone. The dark pigmentation of the stone was correlated with the high content of scytonemin, which was found in all samples.

**Keywords:** black staining; cyanobacteria; scytonemin; limestone

### Introduction

Many historic and artistic objects and buildings are made of stone. Like all materials, stone is subject to deterioration, especially if exposed to outdoor conditions. Among the causes of decay are microbial agents. Biodeterioration, defined as any undesirable change in the properties of a material caused by the vital activities of living organisms, is the consequence of chemical, physical and aesthetic damage (Caneva et al. 2008). When buildings are of architectural or historical importance, the consequence of biological damage is more than economic. Biofilms at the solid/air interface can alter the appearance of the building, accelerate the accumulation of atmospheric pollutants and serve as substrata for the growth of other deteriogens, thereby causing further aesthetic, chemical and physical decay (Crispim et al. 2004; Sanmartín et al. 2011). Thus, the biodeterioration of stone monuments represents a permanent loss of cultural heritage.

This paper reports microbiological research carried out on the external walls of the National Museum of the American Indian Building (NMAI), Washington, DC, USA. The NMAI Building opened in 2004 after several years' construction. It is constructed principally of Monkato Kasota stone, a dolomitic limestone

quarried in Monkato, Minnesota. The stone is generally yellow but some surfaces have orange, dark red and even purplish colouration. Soon after the building was completed, some areas of the external stone surface were covered by black staining, putatively attributed by conservators to microbial growth. In 2007, the masonry surfaces were cleaned using power washing and in 2009, pressure washing was employed. However, both treatments failed to completely remove the staining without also removing the surface of the stone.

Microbial biofilms on outdoor stone are mainly composed by phototrophic microorganisms, in particular cyanobacteria and fungi (Crispim et al. 2004; Gorbushina 2007; Samad and Adhikary 2009). The microflora colonising buildings represents a complex ecosystem, which develops in various ways depending on environmental conditions (eg water availability, period of wetness, substratum orientation and exposure to sunlight) and the physico-chemical properties of the stone. On artistic stone, microorganisms can form coloured patinas. In particular, the resistance to ultraviolet light is generally associated with the production of protective pigments (Garcia-Pichel et al. 1992; Crispim et al. 2004; Sanmartín et al. 2010).

\*Corresponding author. Email: francesca.cappitelli@unimi.it

The aim of the present work was to investigate the deterioration of the stone, specifically the relationships of microorganisms with the stone and to identify the cause of the black staining of the wall surfaces. The detection and identification of the deteriogenic microorganisms and their products are extremely important for the prevention and/or control of microbial colonisation.

## Materials and methods

### *Samples*

Sampling areas were selected by visual inspection of discoloured areas in order to obtain representative samples. Three pieces of limestone with biofilms were collected using a sterile scalpel: sample 2 from the low wall at the north-west corner, sample 5 from an area where runoff from the east roof (near the museum director's balcony) occurred, and sample 7 from the east face below the scupper (Figure 1).

### *Optical microscope observation*

Biomass was rehydrated and examined using a Wild Makroskop M5A stereomicroscope (Heerbrugg, Switzerland) equipped with a Nikon E5600 camera (Chicago, IL, USA). Polished cross-sections were

obtained after embedding samples in a polyester resin (New Basic) and observed under a Wild M3 stereomicroscope and a Leitz Orthoplan microscope equipped with a Leica DC300 camera.

### *Scanning electron microscopy and EDX analysis*

Sample surfaces and cross sections were further characterised by scanning electron microscopy (SEM) using a Philips SEM 505 equipped with an energy-dispersive X-ray spectrometer (EDX). The inner part of the stone cross sections were also analysed in order to provide the elemental composition of the original stone substratum that had not been exposed to the outdoor environment (control samples).

### *DNA extraction and amplification*

Total genomic DNA was extracted in a laminar flow hood as reported by Ausubel et al. (1994) with the follow modifications: no lysozyme was added and four freeze and thaw cycles  $-80^{\circ}\text{C}/70^{\circ}\text{C}$ , for 5 min each were performed before the addition of the proteinase K.

Partial 16S rRNA gene amplification for subsequent denaturing gradient gel electrophoresis (DGGE) analysis was performed for the bacteria with the

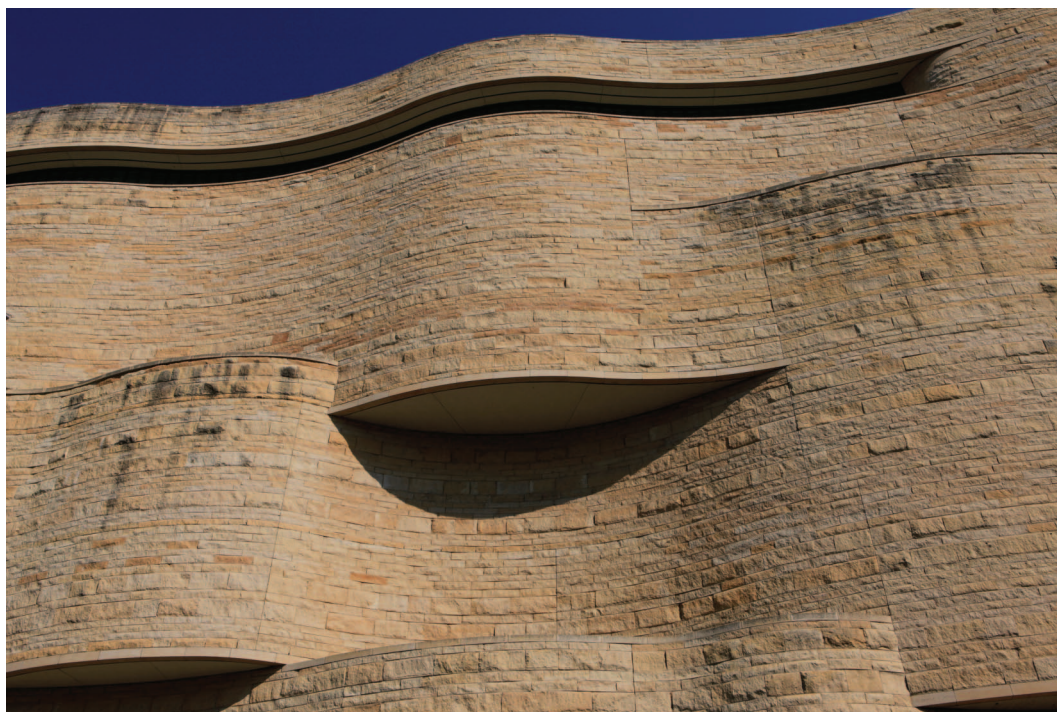


Figure 1. National Museum of the American Indian Building, Washington, DC, USA. The area below the scupper on the east facade of an inner terrace was accessed from the fifth floor from which sample 5 was taken. Image taken by E. Keats Webb, MCI Contract Imaging Specialist.

primer set 357F-GC (CCTACGGGAGGCAGCAG) and 907R (CCGTCAATTCCTTTGAGTTT). The GC clamp was as follows: \*5'-CGCCCGCCGCGCGC GGCGGGCGGGGCGGGGCACGGGGGG-3'. The thermal cycles used for amplification were as follows: 4 min preincubation at 94°C, 10 cycles of 94°C, 61°C, 72°C for 1 min each step, and 20 cycles of 94°C for 30 s, 56°C for 1 min, 72°C for 1 min and a final extension step at 72°C for 10 min (Thermohybrid PCR P × 2 Thermal Cycler).

For fungi, the internal transcribed spacer 1 (ITS1) region, 5.8S rDNA and ITS2 (Chen et al. 2001) were amplified in two steps in a semi-nested procedure with the following primers: ITS4 (TCCTCCGCTTATTGATATGC) and NS5 (AACTTCCCAGGAATTGACGAAG) for the first amplification (White et al. 1990) and ITS1f-GC (CTTGGTCATTTAGAGGAAGTAA) and ITS4 for the second amplification step. The GC clamp was as follows: 5'-CGCCCGCCGCGCGCGCGGGCGGGGCGGGGGCACGGGGGG-3' (Gardes and Bruns 1993).

For algae, partial 18S rRNA gene amplification was performed with the primer set NS1-GC and NS2 as reported by Oros-Sichler et al. (2006) with the annealing temperature modified to 63°C.

Primers CYA359-GC and CYA781R (equimolar mixture between primers CYA781Ra and CYA781Rb) were used for PCR amplification of cyanobacterial 16S rRNA genes as described in Nübel et al. (1997). The thermal cycles used for amplification were as follows: 5 min at 94°C, 35 cycles of 94°C for 45 s, 60°C for 45 s, 72°C for 2 min, and a final extension step at 72°C for 10 min (Thermohybrid PCR P × 2 Thermal Cycler). Aliquots of amplicons were loaded in 1.2% agarose gel in 0.5X TBE buffer (45 mM Tris-borate, 1 mM EDTA) to verify specificity.

### *Denaturing gradient gel electrophoresis (DGGE)*

DGGE was performed using polyacrylamide gel (8% of a 37:1 acrylamide-bisacrylamide mixture in tris acetate EDTA (TAE) 1X buffer, 16 × 10 cm (0.75 mm thick) with a 30–50% denaturant gradient for fungi and eukaryotic algae and a 40–60% denaturant gradient for bacteria and cyanobacteria. Gels were run overnight at 60 V in TAE 1X buffer at 60°C in a DCode apparatus (Bio-Rad, Milan, Italy). Gene fragments were visualised after SYBR<sup>®</sup> Green (Sigma-Aldrich, Milan, Italy) staining by UV transillumination (Gel Doc 2000 apparatus, Bio-Rad, Milan, Italy). Clearly defined bands were cut out from the gel and sequenced at an external facility (Primm, Milan, Italy) with an ABI Prism 3900 Genetic Analyser (Applied Biosystems). The sequences retrieved were blasted against the NCBI database

(<http://www.ncbi.nlm.nih.gov>) and the most probable identification of organisms is given.

### *DGGE profile analyses*

Using DGGE profiles, line plots were generated with ImageJ software (Rasband 2008), and then imported into an Excel<sup>®</sup> file as x/y values. To examine the relative similarities among samples, the matrix of x/y values of DGGE line profiles was analysed by principal component analysis (PCA) using the first two factors, which described most of the variation in the data set. Multivariate investigations were conducted with XLSTAT version 2009.4.07 (Addinsoft, NY) software using the Pearson correlation similarity index. The significance of the PCA model was tested by a cross-validation procedure.

Community profiles were subjected to peak fitting analyses (PeakFit, SPSS, Inc.) to quantify the DNA band positions (peaks representing individual taxonomic units, differentiated by a reference fragment value, Rf) and intensities (peak area representing the abundance of each taxonomic unit). Baselines were subtracted from each line profile using the AutoFit 2nd Deriv Zero routine with the best fit option. After baseline correction, the peaks were resolved with a deconvolution curve fit, which defines a visible peak as one that produces a local maximum in the input data. A standard peak width was assigned to all peaks using the default parameter 'full width at half maximum' that is utilised for fitting Gaussian curves to the peaks. The data matrix containing DNA band positions (peaks representing individual taxonomic units, differentiated by a reference fragment value, Rf) and intensities (peak area representing the abundance of each taxonomic unit) resulted from DGGE fingerprints of total bacterial, cyanobacterial, algal and fungal community of the three samples, were used to estimate diversity indices. The Shannon–Wiener index of diversity (H) was used to compare changes in diversity of microbial communities within the three samples by using the function  $H = -(\sum P_i \log P_i)$ , where  $P_i = n_i/N$ ,  $n_i$  is the peak area, and N is the sum of all peak areas in the curve (Magurran 1988). Evenness (E) was calculated as  $E = H/H_{\max} = H/\ln S$  (35), where S is the number of bands or peaks. Evenness varies between 0 and 1 and gives a measure of the ratio of the observed diversity (H) to the maximum diversity ( $H_{\max} = \ln S$ ) describing the relative abundance of the different taxa. Simpson's index of dominance ( $D = \sum p_i^2$ ) estimates the probability that any two individuals drawn from a community belong to different species. It is often expressed as  $1/D$  so that an increase in the index reflects an increase in diversity (Magurran 1988). Richness was calculated as the

number of unique DGGE bands identified by the PeakFit analysis and it represents the number of taxa per samples. Total abundance is the sum of all peak areas in the profile, used to describe the abundance of taxa within a sample. The results were expressed in units of number of taxa.

### Pigment analysis

Samples were treated with 20 ml of acetone in an ultrasound bath for 15 min and the resulting yellow solution was decanted in a flask. The organic solutions, collected from three subsequent extractions, were filtered through a sintered glass filter and the solvent evaporated at reduced pressure. After extraction, the resulting material was analysed by UV-visible spectrometry (Thermo evolution 500 UV-visible

spectrophotometer) and scytonemin quantified from the recorded spectra in acetone using a specific extinction coefficient  $112.6 \text{ Lg}^{-1} \text{ cm}^{-1}$  at 384 nm (Garcia-Pichel et al. 1992). Scytonemin was detected by electrospray ionisation mass spectrometry (ESI-MS)  $m/z [\text{M-H}]^- 543$ .

### Results

#### Stereomicroscope, optical and electron microscope observation of the black staining

Using a stereomicroscope, the following was observed: an irregular alteration of the surface following the boundary crystals, dark brown in colour in sample 2 (Figure 2a); an alteration covering a larger surface area in sample 5 than in sample 2 (Figure 2b); the presence of black material irregularly distributed on

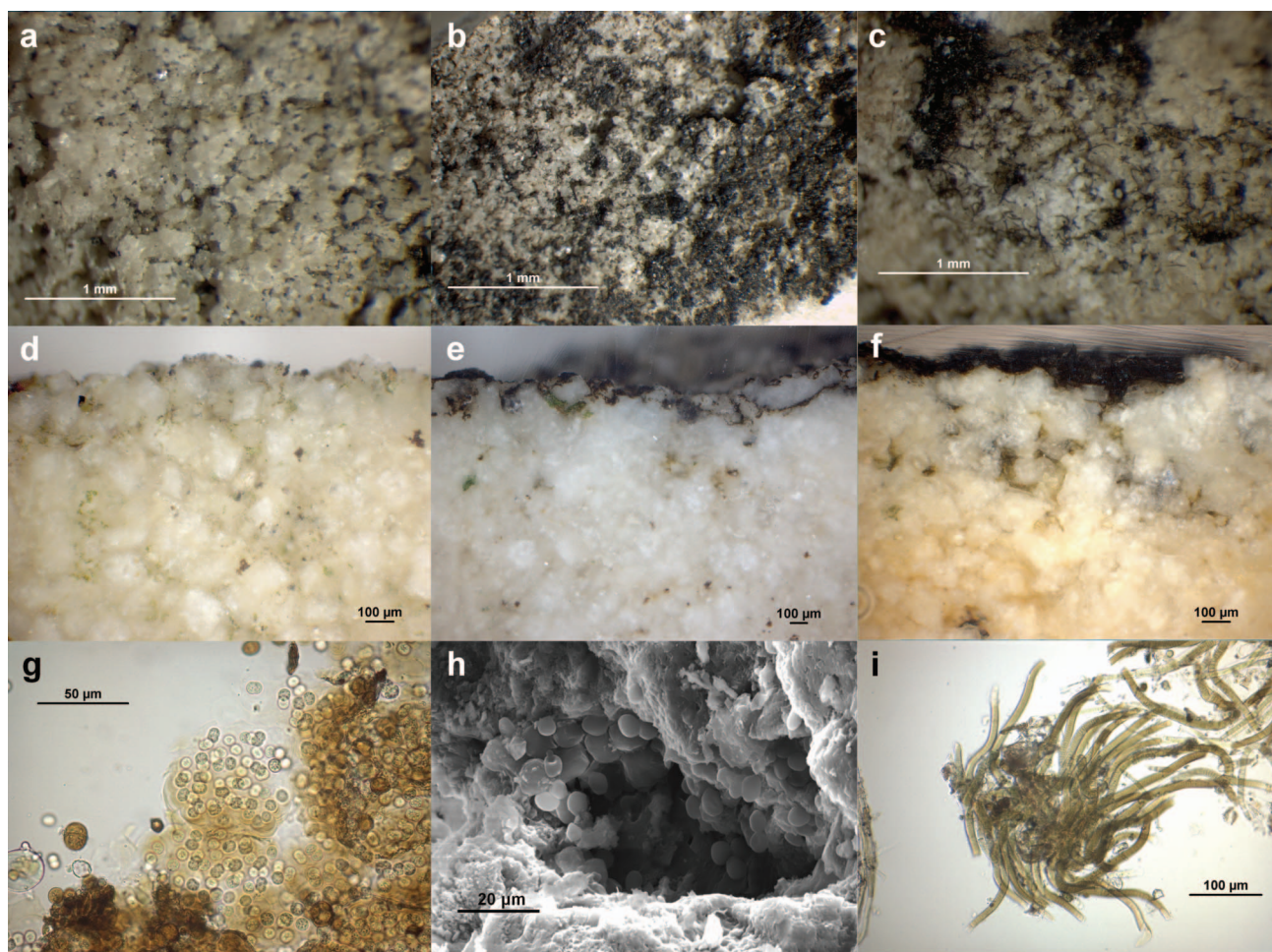


Figure 2. Microscopic analysis of the three discoloured stone specimens. Micrographs of dark material irregularly distributed on the surface of samples 2 (a), 5 (b) and 7 (c). Polished cross sections of samples 2 (d), 5 (e) and 7 (f) show an appreciable endolithic growth of photosynthetic microorganisms. Optical (g, i) and electron micrographs (h) show that in all three samples cyanobacteria were the predominant microorganisms. In particular, the dark material on the surface of sample 2 (g) is attributed to biofilm composed mainly of *Gloeocapsa*-like cells while the examination of fresh slides in sample 7 (i) show a clear prevalence of a filamentous cyanobacterium belonging to the genus *Lyngbya* as no false branching was observed.

the surface, with localised concentrations in sample 7 (Figure 2c).

Optical and SEM observations confirmed the presence of microbial cells forming a biofilm. The observations showed that cyanobacteria were the predominant microorganisms in all three samples, although different species were observed (Figure 2g–i). Optical microscopy of the dark material on the surface of samples 2 and 5 showed the presence of cyanobacteria with the predominance of colonies of *Gloeocapsa* sp., which had coloured sheaths (Figure 2g). The other cyanobacteria identified belonged to the genera *Aphanocapsa* and *Chroococcus*. The examination of fresh slides in sample 7 showed a clear prevalence of a filamentous cyanobacterium with a dark sheath belonging to the genus *Lyngbya* (Figure 2i). Other cyanobacteria, viz. *Calothrix* sp., *Pseudoanabaena* sp. and *Aphanocapsa* sp. were occasionally observed.

The observation of cross-sections showed that cyanobacteria developed not only on the surface but also underneath, reaching a maximum depth of about 1 mm. Greater penetration into the stone was generally associated with thicker surface colonisation and along pre-existing microcracks and fissures. In particular, the polished cross sections of samples 2 (Figure 2d) and 5 (Figure 2e) showed appreciable development of photosynthetic microorganisms within the stone down to a depth of *ca* 1 mm. In sample 5, the presence of endolithic growth was higher next to the more colonised areas on the stone surface. Polished cross sections of sample 7 showed the microorganisms on the surface formed a layer reaching 200  $\mu\text{m}$  of thickness in the clusters. In addition, cells penetrated into the stone to an average depth of *ca* 600  $\mu\text{m}$  (Figure 2f), although some cyanobacterial cells reached a depth of 1 mm.

SEM of stone embedded in a polymer matrix showed an endolithic biofilm of cells below the surface (Figure 2h). SEM observations showed the network of filaments of *Lyngbya* sp. firmly attached to the stone. In some areas particulate matter and pollen adhered to the sheaths of the cyanobacteria.

#### Analysis of the total community

To obtain more detailed information about the microbial communities present on the samples, the composition of the total community was determined by DGGE analysis coupled with a partial sequencing of the 16S rRNA genes for bacteria, cyanobacteria and plastids, the ITS region for fungi, and 18S rRNA genes for fungi and eukaryotic algae. PCR-amplifiable DNA was recovered from all samples. Even though the number of discernible bands differed among samples, 16S rRNA gene amplification showed a total of 33 and 16 distinct bands in the DGGE gels for bacteria and

cyanobacteria, respectively, 20 for the fungal ITS amplification, while for the 18S rRNA gene only 6 bands were seen. The DGGE profiles of samples 2, 5 and 7 revealed there was overall high molecular diversity.

The DGGE profiles obtained were analysed to evaluate the diversity indices of the different samples and the similarities among the communities of the three specimens, with reference to cyanobacteria (Figure 3), the total prokaryotic community, and fungi and algae. Diversity indices calculated using band position and intensities of the DGGE profiles indicated that sample 7 showed the lowest genetic diversity of the microbial community and sample 5 the highest (Table 1). The same trend applied to species richness.

Principal component analysis showed that both in the case of the total community, including both prokaryotes and eukaryotes, and the case of the bacterial community alone, the communities of the samples were different.

The samples were also characterised by sequencing the DGGE bands for bacteria, cyanobacteria, fungi

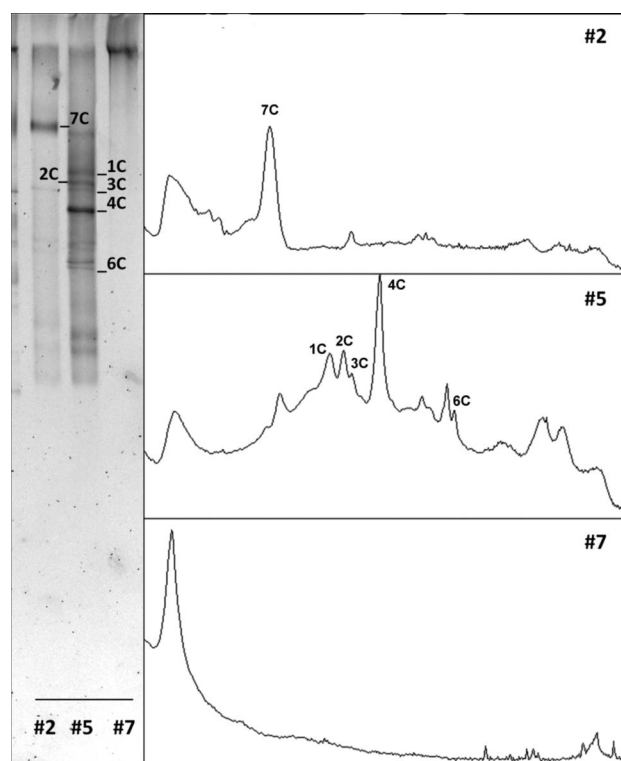


Figure 3. DGGE and line plot profiles of the three specimens obtained from the 16S rRNA gene of cyanobacteria and plastids. Label bands and the corresponding peaks denote predominant DNA bands that were sequenced for identification of cyanobacterial species (Table 2). The line plot profiles obtained with ImageJ software revealed that the cyanobacterial community composition of the three collected samples was different.

and algae. Sequences were obtained for the microbial community by BLAST in the NCBI database and are reported in Table 2. It was possible to obtain homologies to sequences of known microorganisms ranging from 92% to 99%. In the case of the cyanobacterial community analyses, different bands presented very low levels of homology with those in DNA databanks.

Table 1. Diversity indices based on DGGE data.

	Sample 2	Sample 5	Sample 7
Shannon–Wiener diversity index	2.986903	3.555933	2.61909
Species richness (S)	42	59	29
Total abundance	19945	88046	17774
Simpson diversity index (1/D)	10.94254	27.10257	8.309187
Evenness	0.799135	0.872079	0.777802

The data matrix contained DNA band positions (peaks representing individual taxonomic units, differentiated by a reference fragment value, RF) and intensities (peak area representing the abundance of each taxonomic unit) resulting from DGGE fingerprints of total prokaryotic and eukaryotic microbial communities. The data matrix was composed of 91 rows (where 91 is the number of peaks obtained from peak fitting analyses of the total community profiles) and three columns, one for each sample. Results are expressed in units of number of taxa.

Table 2. Identification of gene sequences isolated from DGGE profiles.

Band	Accession number	Closest relative	% Similarity	Sample 2	Sample 5	Sample 7
1C	EU434900.1	Uncultured cyanobacterium from Oscillatoriales	98		X	
6C	FJ028679.1	Uncultured cyanobacterium	96		X	
7C	EF522240.1	Uncultured chlorophyte	98	X		
4C	FJ891024.1	Uncultured cyanobacterium	98		X	
3C	FN298109.1	Uncultured cyanobacterium	98	X	X	
2C	FN298109.1	Uncultured cyanobacterium	98		X	
4A	AF513369.1	<i>Myrmecia</i> sp. H1VF1	98	X	X	X
5A	FJ790653.1	Uncultured Trebouxiophyceae	97	X		
5F	FM991735.1	<i>Epicoccum nigrum</i>	99		X	
12F	AJ972830.1	Ascomycete sp. MA 4698	99		X	
13F	AJ972860.1	<i>Capnobotryella</i> sp. MA 4775	99		X	
16F	DQ525508.1	<i>Pleopsidium</i> sp.	95	X		
21F	DQ534198.1	<i>Cladonia</i> sp.	94	X		
22F		High quality DNA sequence but no match in the databank			X	
23F		High quality DNA sequence but no match in the databank			X	
1B	AM230699.2	<i>Calothrix desertica</i> PCC 7102	99			X
2B	GU271789.1	Uncultured <i>Candidatus</i> sp.	92			X
3B	AY571796.1	Uncultured Acidobacteria bacterium	94	X		
5B	HQ189006.1	Uncultured cyanobacterium	98	X	X	
10B	AB374378.1	Uncultured endolithic bacterium	98	X		
11B	DQ366016.1	Uncultured <i>Deinococcus</i> sp.	99	X		
12B	EF522240.1	Uncultured chlorophyte	98	X		
15B	EU527174.1	Uncultured bacterium	99		X	
16B	EF507900.1	<i>Spirosoma rigui</i>	98	X	X	
17B	EU434900.1	Uncultured Oscillatoriales cyanobacterium	98	X	X	
18B	GU124813.1	<i>Synechococcus</i> sp. HH-1	98		X	
19B	FJ805854.1	Uncultured <i>Chroococciopsis</i> sp.	98		X	

The total bacterial, cyanobacterial, algal and fungal communities were investigated. A cross indicates that the band was present in the sample. C = cyanobacteria; B = bacteria; A = algae; F = fungi.

Phylogenetic affiliations of excised DGGE bands were represented by the phyla Cyanobacteria, Chlorophyta, Ascomycota, Acidobacteria, Bacteroidetes and Deinococcus-Thermus. Two sequences did not show any similarity to reported sequences in databases, thus they may be novel sequences, which would be worthy of further study.

#### EDX analysis

Energy-dispersive X-ray spectroscopy analysis showed the same elemental composition (C, O, Mg, Al, Si, K, Ca, Fe) in the control as well as in stained and unstained areas of the three samples. The percentage composition of C and O in the colonised areas was higher compared to the uncolonised stone. Furthermore, higher levels of Mg, Al, Si, K, Ca and Fe were found in unstained areas. EDX spectra of sample 7 are shown in Figure 4.

#### Pigment analysis

The presence of scytonemin was confirmed in extracts by mass spectrometry. Absolute and normalised surface amounts of scytonemin in all samples are reported

in Table 3. It should be noted that UV absorbance at 384 nm might not solely be related to scytonemin; a small contribution may also be ascribed to carotenoids, aliphatic molecules that might also be extracted by acetone.

## Discussion

The distribution of black staining on the NMAI building was examined in April 2010. Soiling was clearly related to preferential water paths where water runs down the surfaces and it was present on the external walls facing all exposures. For these reasons, the black staining was attributed to biological colonisation. In this case study, molecular and microscopic examination revealed the endolithic biofilm was predominantly composed of cyanobacteria. Cyanobacteria are very common on monuments, often being the first colonisers in the succession of microbial populations on stone (Macedo et al. 2009). Importantly, heterotrophic bacteria and fungi can grow on secreted

metabolites of cyanobacteria or photosynthetic biomass (Ortega-Morales 2006).

Cyanobacteria damage stone due to the production of inorganic and organic metabolic products, in particular acids, some of which have chelating abilities (Ramirez et al. 2010). In addition, their hygroscopic slimy sheaths embed dirt and pollutants and exert mechanical stress on the mineral structure due to increased water retention, causing diminished crystal coherence and an alteration of pore size and distribution, together with modifications in water circulation patterns (Albertano et al. 2000; Crispim et al. 2004; Di Pippo et al. 2011). It is well known that the discolouration caused by cyanobacteria allows the organisms to withstand high illumination and UV levels (Golubic et al. 1981; Sanmartín et al. 2010).

In this study the cyanobacteria were identified based on morphology as belonging to the genera *Gloeocapsa*, *Lyngbya*, *Aphanocapsa*, *Chroococcus*, *Calothrix*, and *Pseudoanabaena*. The cyanobacterial genera colonising the NMAI building are ubiquitous and therefore their presence is not strictly related to the stone type. Some cyanobacteria penetrated into the stone. In extreme habitats, as on outdoor stone surfaces, endolithic growth provides mineral nutrients and protects cells from low temperature, UV radiation and desiccation (Giacomucci et al. 2011). Molecular analysis of the cyanobacterial community showed the presence of *Calothrix desertica* (99% similarity), an organism that has been identified in a heavy metal hyporheic area in Montana, USA (Feris et al. 2003) and the extremophile *Chroococcidiopsis* sp. (98% similarity) that is found growing in rocks in hot and cold deserts. *Chroococcidiopsis* is highly desiccation and radiation resistant (Billi et al. 2000). Most of the information available on the systematics of cyanobacteria has emerged from identifications made only on the basis of morphology, a trait that generally does not correlate well with phylogeny (de los Ríos et al. 2007). Microscopic analyses tend to underestimate the biodiversity of cyanobacteria due to the high variability in morphology reflecting different environmental and growth conditions (Zapomelová et al. 2008). The fact that most of the cyanobacterial sequence homologues failed to identify the genera is not surprising as DNA databanks comprise mainly aquatic cyanobacteria, suggesting that many cyanobacterial species remain to be discovered (Gaylarde et al. 2004; Cappitelli et al. 2009). In addition, significant differences in cyanobacterial diversity (16S rRNA genes recovered) within phototrophic biofilms evaluated by DGGE, relies on the application of different DNA extraction methods (Ferrera et al. 2010). Molecular methods of DNA analysis might fail to detect the presence of cyanobacteria with thick sheaths, which

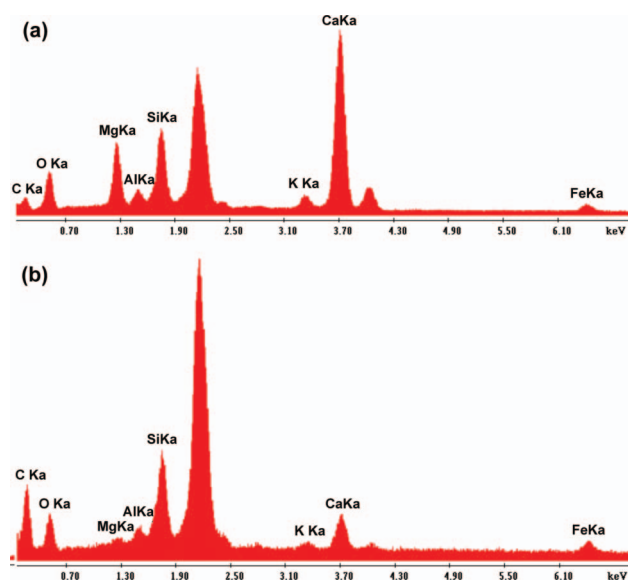


Figure 4. EDX spectra of unstained (a) and stained (b) areas of sample 7.

Table 3. Results of pigment analysis.

	Amount extracted (mg)	Amount extracted/altered surface (mg cm <sup>-2</sup> )	c (mg ml <sup>-1</sup> )
Sample 2	0.5	0.5	0.00095
Sample 5	2	0.3	0.00718
Sample 7	3	0.5	0.0128

Scytonemin was acetone extracted from phototrophic biofilms and quantified spectrophotometrically using the specific extinction coefficient 112.6 Lg<sup>-1</sup> cm<sup>-1</sup> at 384 nm.

were conspicuous on microscopic observation (Garcia-Pichel et al. 2001). Several studies demonstrate that significant components of cyanobacterial biodiversity can be underestimated when a single method for community description is used (Garcia-Pichel et al. 2001; Foster et al. 2009). Thus, for a more holistic picture of cyanobacterial diversity, combined molecular/morphological studies are needed.

It was interesting to note that most of the cyanobacteria retrieved were characteristic of lithic environments (eg band 6C) and included two sequences (bands 1C and 17B) with 98% similarity with phototrophic microbial communities colonising a single natural shelter containing prehistoric paintings (Portillo et al. 2009) and two sequences (bands 2C and 3C, 98% similarity) with microbial communities from the Roman Necropolis of Carmona tombs (accession no. FN298109.1, unpublished data). Other sequences were related to arid environments (bands 4C and 5B, 98% similarity) (Lacap et al. 2011).

Molecular analysis of the total community showed that eukaryotic algae, fungi and heterotrophic bacteria were also present. Green algae from the Trebouxiophyceae were detected in all samples (bands 4A and 5A). This family was found in desert soil by Lewis and Lewis (2005) and in hypolithic stone niches (Wong et al. 2010). Members of the Ascomycota were found in samples 2 and 5, and black fungi in sample 5. Many black fungi, such as *Epicoccum nigrum* and *Capnobotryella* sp., physically attack rock and cause aesthetic and structural damage on artistic stone (Saiz-Jimenez 1995; Sterflinger 2000; Sert et al. 2007). *Pleopsidium* (band 16F) and *Cladonia* (band 21F) are lichen-forming ascomycetes (Hibbett et al. 2007), indicating that lichens were also present on the lithic surface.

Acidobacteria and *Deinococcus*, which have been found on other monuments, eg Angkor temples of Angkor Thom and Bayon in Cambodia (Lan et al. 2010), were found in samples 2 and 7 and sample 2, respectively. Some of the bacteria found showed an endolithic habitat (band 10B), while others were found in cold environments (bands 15B and 16B) (Baik et al. 2007; Liu et al. 2009).

Diversity indexes indicated diversity in species and richness among the samples despite the stone of the three samples being the same limestone. This fact highlights the important role played by environmental conditions and substratum orientation in determining microbial community structure (Macedo et al. 2009).

EDX analysis suggested that the origin of the black staining on the NMAI building was not chemical, but biological in nature as control, stained and unstained areas showed similar elemental composition and the percentage composition of C and O in colonised areas

was higher compared to uncolonised stone. It is likely that the presence of a thick phototrophic biofilm on the stained areas masked the high level of Mg, Al, Si, K, Ca and Fe measured on the unstained ones. As sulfur dioxide pollution is produced when sulfur containing fuels are burned, the absence of high S peaks in the EDX spectra indicated that the sites sampled were low in this type of urban pollution. The presence of cyanobacteria with dark brown sheaths was subjected to solvent extraction and analysis. The discolouration was ascribed to the presence of a sheath yellow-brown pigment, scytonemin, that acts as ultraviolet sunscreen in habitats exposed to intense solar radiation. This pigment may also provide significant protection to microorganisms other than cyanobacteria (Garcia-Pichel and Castenholz 1991). Scytonemin appears to be a single compound identified in several cyanobacterial species, eg *Gloeocapsa* species (Lewin 2006). Scytonemin production provides an adaptive strategy to protect cells against short-wavelength solar irradiance and can mask the normal intracellular complement of pigments, thus making the biofilms look black (Lewin 2006). According to Lewin (2006) most black discolouration of limestone rocks and whitewashed walls is attributable to cyanobacteria of the genus *Gloeocapsa*, which were observed as the dominant algae in samples 2 and 5. Both *Gloeocapsa* and *Lyngbya* spp., the latter being the predominant cyanobacterial species of sample 7, are known to grow on stone substrata (Crispim et al. 2004) and both synthesise scytonemin (Balskus et al. 2011). As recorded in the stone conservation literature, *Lyngbya* is frequently detected on stone monuments in temperate and tropical climates, and sometimes it is one of the dominant colonisers (Tomaselli et al. 2000; Crispim et al. 2003; Deepa et al. 2011; Gaylarde et al. 2012). The content of scytonemin has been attributed to the dark appearance of the biofilm (Gaylarde et al. 2007). In this paper an index is proposed that is the ratio between the weight of extracted scytonemin and the altered surface area. This type of index, related to chlorophyll *a*, has been previously used to express granite bioreceptivity (Prieto and Silva 2005; Prieto et al. 2006). The highest genetic diversity and species richness of sample 5 could be explained by the lowest scytonemin content per area of altered surface. In addition, sample 5 showed an appreciable endolithic development of phototrophic biofilm, which might hinder pigment extraction. This is a rapid and simple index to obtain and may be useful to conservators when dealing with the cleaning treatment.

The need to clean the NMAI building has been perceived as being critical for its proper conservation. However, this type of treatment is more difficult if photosynthetic microorganisms, such as those

retrieved in this study, penetrate deeply into the stone. Such endolithic microorganisms cannot be reached by mechanical cleaning, and if some cells or colonies survive biocide treatments they could rapidly regrow (Gladis et al. 2010). In addition, it must be remembered that dead cells remaining inside the stone could also be used as source of nourishment for heterotrophic microorganisms. A careful application of biocides that penetrate the inner colonised stone should avoid rapid recolonisation of the stone surface.

### Acknowledgements

The authors thank Dr Robert J. Koestler and Dr Paula DePriest of the Smithsonian's Museum Conservation Institute for the opportunity to obtain the samples used in this study from the Smithsonian's National Museum of the American Indian Building.

### References

- Albertano P, Bruno L, Bellezza S, Paradossi G. 2000. Polysaccharides as a key step in stone bioerosion. Proceedings of the 9th International Congress on Deterioration and Conservation of Stone. Amsterdam: Elsevier. p. 425–432.
- Ausubel FM, Brent R, Kingston RE, Moore DD, Seidman JG, Smith JA, Struhl K. 1994. Current protocols in molecular biology. Supplement 27, Unit 2.3.1 to 2.3.7. New York (NY): John Wiley & Sons, Inc.
- Baik KS, Kim MS, Park SC, Lee DW, Lee SD, Ka JO, Choi SK, Seong CN. 2007. *Spirosoma rigui* sp. nov., isolated from fresh water. *Int J Syst Evol Microbiol* 57:2870–2873.
- Balskus EP, Case RJ, Walsh CT. 2011. The biosynthesis of cyanobacterial sunscreen scytonemin in intertidal microbial mat communities. *FEMS Microbiol Ecol* 77:322–332.
- Billi D, Friedmann EI, Hofer KG, Caiola MG, Ocampo-Friedmann R. 2000. Ionizing-radiation resistance in the desiccation-tolerant cyanobacterium *Chroococcidiopsis*. *Appl Environ Microbiol* 66:1489–1492.
- Caneva G, Nugari MP, Salvadori O, editors. 2008. Plant biology for cultural heritage. biodeterioration and conservation. Los Angeles (CA): The Getty Conservation Institute. 408 pp.
- Cappitelli F, Abbruscato P, Foladori P, Zanardini E, Ranalli G, Principi P, Villa F, Polo A, Sorlini C. 2009. Detection and elimination of cyanobacteria from frescoes: the case of the St Brizio Chapel (Orvieto Cathedral, Italy). *Microb Ecol* 57:633–639.
- Chen YC, Eisner JD, Kattar MM, Rassoulouian-Barrett SL, Lafe K, Bui U, Limaye AP, Cookson BT. 2001. Polymorphic internal transcribed spacer region 1 DNA sequences identify medically important yeasts. *J Clin Microbiol* 39:4042–4051.
- Crispim CA, Gaylarde CC, Gaylarde PM. 2004. Biofilms on church walls in Porto Alegre, RS, Brazil, with special attention to cyanobacteria. *Int Biodeterior Biodegr* 54:121–124.
- Crispim CA, Gaylarde CC, Gaylarde PM, Copp J, Neilan BA. 2003. Molecular biology for the investigation of cyanobacterial populations on historic buildings in Brazil. In: Saiz-Jimenez C, editor. Molecular biology and cultural heritage. Lisse (the Netherlands): Balkema Publishers. p. 141–144.
- de los Ríos A, Grube M, Sancho LG, Ascaso C. 2007. Ultrastructural and genetic characteristics of endolithic cyanobacterial biofilms colonizing Antarctic granite rocks. *FEMS Microbiol Ecol* 59:386–395.
- Deepa P, Jeyachandran S, Manoharan C, Vijayakumar S. 2011. Survey of epilithic cyanobacteria on the temple walls of Thanjavur district, Tamilnadu, India. *World J Sci Technol* 1:28–32.
- Di Pippo F, Bohn A, Cavalieri F, Albertano P. 2011. <sup>1</sup>H-NMR analysis of water mobility in cultured phototrophic biofilms. *Biofouling* 27:327–336.
- Feris K, Ramsey P, Frazar C, Moore JN, Gannon JE, Holben WE. 2003. Differences in hyporheic-zone microbial community structure along a heavy-metal contamination gradient. *Appl Environ Microbiol* 69:5563–5573.
- Ferrera I, Massana R, Balagué V, Pedrós-Alió C, Sánchez O, Mas J. 2010. Evaluation of DNA extraction methods from complex phototrophic biofilms. *Biofouling* 26:349–357.
- Foster JS, Green SJ, Ahrendt SR, Golubic S, Reid RP, Hetherington KL, Bebout L. 2009. Molecular and morphological characterization of cyanobacterial diversity in the stromatolites of Highborne Cay, Bahamas. *ISME J* 3:573–587.
- García-Pichel F, Castenholz RW. 1991. Characterization and biological implications of scytonemin, a cyanobacterial sheath pigment. *J Phycol* 27:395–409.
- García-Pichel F, López-Cortés A, Nübel U. 2001. Phylogenetic and morphological diversity of cyanobacteria in soil desert crusts from the Colorado plateau. *Appl Environ Microbiol* 67:1902–1910.
- García-Pichel F, Sherry ND, Castenholz RW. 1992. Evidence for an ultraviolet sunscreen role of the extracellular pigment scytonemin in the terrestrial cyanobacterium *Chlorogloeopsis* sp. *Photochem Photobiol* 56:17–23.
- Gardes M, Bruns TD. 1993. ITS primers with enhanced specificity for basidiomycetes-applications to the identification of mycorrhizae and rusts. *Mol Ecol* 2:113–118.
- Gaylarde CC, Ortega-Morales BO, Bartolo-Pérez P. 2007. Biogenic black crusts on buildings in unpolluted environments. *Curr Microbiol* 54:162–166.
- Gaylarde CC, Gaylarde PM, Copp J, Neilan B. 2004. Polyphasic detection of cyanobacteria in terrestrial biofilms. *Biofouling* 20:71–79.
- Gaylarde CC, Rodríguez CH, Navarro-Noya YE, Ortega Morales BO. 2012. Microbial biofilms on the sandstone monuments of the Angkor Wat complex, Cambodia. *Curr Microbiol* 64:85–92.
- Giacomucci L, Bertocello R, Salvadori O, Martini I, Favaro M, Villa F, Sorlini C, Cappitelli F. 2011. Microbial deterioration of artistic tiles from the facade of the Grande Albergo Ausonia and Hungaria (Venice, Italy). *Microb Ecol* 62:287–298.
- Gladis F, Eggert A, Karsten U, Schumann R. 2010. Prevention of biofilm growth on man-made surfaces: evaluation of anti-algal activity of two biocides and photocatalytic nanoparticles. *Biofouling* 26:89–101.
- Golubic S, Friedmann EI, Schneider J. 1981. The lithobiontic ecological niche, with special reference to microorganisms. *J Sediment Petrol* 51:475–478.
- Gorbushina AA. 2007. Life on the rocks. *Environ Microbiol* 9:1613–1631.
- Hibbett DS, Binder M, Bischoff JF, Blackwell M, Cannon PF, Eriksson OE, Huhndorf S, James T, Kirk PM, Lücking R, et al. 2007. A higher-level phylogenetic classification of the Fungi. *Mycol Res* 111:509–547.

- Lacap DC, Warren-Rhodes KA, McKay CP, Pointing SB. 2011. Cyanobacteria and chloroflexi-dominated hypolith colonization of quartz at the hyper-arid core of the Atacama Desert, Chile. *Extremophiles* 15:31–38.
- Lan W, Li H, Wang WD, Katayama Y, Gu JD. 2010. Microbial community analysis of fresh and old microbial biofilms on Bayon temple sandstone of Angkor Thom, Cambodia. *Microb Ecol* 60:105–115.
- Lewin RA. 2006. Black algae. *J Appl Phycol* 18:699–702.
- Lewis LA, Lewis PO. 2005. Unearthing the molecular phylodiversity of desert soil green algae (Chlorophyta). *Syst Biol* 54:936–947.
- Liu Y, Yao T, Jiao N, Kang S, Xu B, Zeng Y, Huang S, Liu X. 2009. Bacterial diversity in the snow over Tibetan Plateau Glaciers. *Extremophiles* 13:411–423.
- Macedo MF, Miller A, Dionísio A, Saiz-Jimenez C. 2009. Biodiversity of cyanobacteria and green algae on monuments in the Mediterranean Basin: an overview. *Microbiology* 155:3476–3490.
- Magurran AE. 1988. Ecological diversity and its measurement. London (UK): Chapman & Hall. 179 pp.
- Nübel U, Garcia-Pichel F, Muyzer G. 1997. PCR primers to amplify 16S rRNA genes from cyanobacteria. *Appl Environ Microbiol* 63:3327–3332.
- Oros-Sichler M, Gomes NCM, Neuber G, Smalla K. 2006. A new semi-nested PCR protocol to amplify large 18S rRNA gene fragments for PCR–DGGE analysis of soil fungal communities. *J Microbiol Methods* 65:63–75.
- Ortega-Morales BO. 2006. Cyanobacterial diversity and ecology on historic monuments in Latin America. *Rev Latinoam Microbiol* 48:188–195.
- Portillo MC, Alloza R, Gonzalez JM. 2009. Three different phototrophic microbial communities colonizing a single natural shelter containing prehistoric paintings. *Sci Total Environ* 407:4876–4881.
- Prieto B, Silva B. 2005. Estimation of the potential bioreceptivity of granitic rocks from their intrinsic properties. *Int Biodeterior Biodegr* 56:206–215.
- Prieto B, Silva B, Aira N, Álvarez L. 2006. Toward a definition of a bioreceptivity index for granitic rocks: Perception of the change in appearance of the rock. *Int Biodeterior Biodegr* 58:150–154.
- Ramirez M, Hernandez-Marine M, Novelo E, Roldan M. 2010. Cyanobacteria-containing biofilms from a Mayan monument in Palenque, Mexico. *Biofouling* 26:399–409.
- Rasband W. 2008. ImageJ 1997–2007. Bethesda (MD): US National Institutes of Health.
- Saiz-Jimenez C. 1995. Microbial melanins in stone monuments. *Sci Total Environ* 167:272–286.
- Samad LK, Adhikary SP. 2009. Cyanobacteria and microalgae on building facades and stone surface of monuments – an ecophysiological prospective. In: Khattar JIS, Singh DP, Kaur G, editors. *Algal biology and biotechnology*. New Delhi (India): I.K. International Publishers. p. 41–56.
- Sanmartín P, Aira N, Devesa-Rey R, Silva B, Prieto B. 2010. Relationship between color and pigment production in two stone biofilm-forming cyanobacteria (*Nostoc* sp. PCC 9104 and *Nostoc* sp. PCC 9025). *Biofouling* 26:499–509.
- Sanmartín P, Villa F, Silva B, Cappitelli F, Prieto B. 2011. Color measurements as a reliable method for estimating chlorophyll degradation to phaeopigments. *Biodegradation* 22:763–771.
- Sert HB, Sömbül H, Sterflinger K. 2007. Microcolonial fungi from antique marbles in Perge/Side/Termessos (Antalya/Turkey). *Antonie Van Leeuwenhoek* 91:217–227.
- Sterflinger K. 2000. Fungi as geological agents. *Geomicrobiol J* 17:97–124.
- Tomaselli L, Lamenti G, Bosco M, Tiano P. 2000. Biodiversity of photosynthetic micro-organisms dwelling on stone monuments. *Int Biodeterior Biodegr* 46:251–258.
- White TJ, Bruns T, Lee S, Taylor J. 1990. Amplification and direct sequencing of fungal ribosomal RNA genes for phylogenetics. In: Innis MA, Gelfand DH, Sninsky JJ, White TJ, editors. *PCR protocols, a guide to methods and applications*. San Diego (CA): Academic Press. p. 315–322.
- Wong FKY, Lacap DC, Lau MCY, Aitchison JC, Cowan DA, Pointing SB. 2010. Hypolithic microbial community of quartz pavement in the high-altitude tundra of central Tibet. *Microb Ecol* 60:730–739.
- Zapomelová E, Hrouzek P, Reháková K, Sabacká M, Stibal M, Caisová L, Komárková J, Lukesová A. 2008. Morphological variability in selected heterocystous cyanobacterial strains as a response to varied temperature, light intensity. *Folia Microbiol* 53:333–341.